Supplementary Information (SI) for Analyst.

Supporting Information

Detection of Carbapenemase-Mediated Antimicrobial Resistance using Surface-Enhanced Raman Scattering

Ziying Wang [a‡], Hridaynath Bhattacharjee [a‡], Mitchell A. Jeffs [b‡], Rachel A. V. Gray [b], Yazan Bdour [a], Aristides Docoslis [a], Christopher T. Lohans [b]*, and Carlos Escobedo [a]*

[a] Department of Chemical Engineering, Queen's University, Kingston, Ontario, Canada

[b] Department of Biomedical and Molecular Sciences, Queen's University, Kingston, Ontario, Canada

[‡] Contributed equally

Table of Contents

Experimental Section

Reagents and Proteins

Recombinant class A β-lactamase KPC-2 and class D β-lactamase OXA-48 were produced in *Escherichia coli* BL21(DE3) transformed with previously described expression vectors.[1, 2] Transformant colonies were cultured overnight in 2TY media (16 g/L tryptone, 5 g/L NaCl, 10 g/L yeast extract, supplemented with appropriate selection antibiotic) at 37 °C, 200 rpm. Overnight cultures were used to inoculate (1%) fresh 2TY media (with appropriate selection antibiotic), which was then incubated at 37 °C, 200 rpm until the OD_{600} reached 0.5-0.6. Production of OXA-48 and KPC-2 was induced with the addition of 0.1 mM IPTG, and the cultures were then incubated for 16-18 h at 18 °C. Cells were harvested by centrifugation, then the pellet was resuspended in 2.5 mL BugBuster protein extraction reagent (Novagen) containing 1 mg DNase I (Sigma Aldrich). The mixture was incubated on ice for 10 min, then cellular debris was pelleted by centrifugation at 20,000 rpm for 30 min at 4 °C (Sorvall RC6+ centrifuge). The supernatant was passed through 0.45 μm and 0.22 μm filters, then loaded onto a 1 mL HisTrap column (Cytiva). After washing with buffer A (50 mM HEPES, 500 mM NaCl, 20 mM imidazole, pH 7.4), proteins were eluted using buffer B (50 mM HEPES, 500 mM NaCl, 500 mM imidazole, pH 7.4). After assessing protein purity by SDS-PAGE, purified proteins were buffer exchanged into 50 mM HEPES, 500 mM NaCl, pH 7.5 using Vivaspin Turbo 4 (10,000 MWCO) centrifugal filters. Final protein yields were quantified using UV-Vis spectrophotometry, and aliquots were stored at −80 °C.

Meropenem (Glentham Life Sciences) was used at a concentration of 10 mg/L across assays using purified β-lactamases and β-lactamase-producing bacteria. *E. coli* BW25113 (National BioResource Project) was used as a representative non-carbapenemase-producing bacterium, and *E. coli* BW25113 transformed with pACYC184-KPC-2 was used as a model carbapenemase-producing organism.[3]

SERS nanostructure

Gold-based SERS substrates (Ocean Insight-RAM-SERS-AU-5) were purchased from Ocean Optics (Orlando, FL, USA).[4] The substrate is a SERS active circular area with a diameter of 5.5 mm, featuring densely packed Au nanoparticles on paper, fixed on a 25 mm × 75 mm borosilicate glass (see Figure S1b). Analyte solution (10 μL; 10 mg/L) was applied to the active area followed by drying for about 5 min at room temperature. After securing the substrate with the sample holder, the SERS spectra were obtained.

Data acquisition of Raman spectra

An IDRaman micro-Raman spectroscopy system (Ocean Optics) featuring a 785 nm solid-state laser was utilized for sample excitation (see Figure S1a).[5] A 10× microscope was utilized to examine the surface of the SERS-active substrate. A laser power of 10.7 mW and 5 s collection time was used for data acquisition.

Raman signal analysis

The obtained SERS spectra were processed by OceanView software to remove background fluorescence and to correct the baseline. For each sample, 20 spectral datasets were collected from various locations on the substrate, and an average spectrum was obtained and plotted using Origin Pro software. Peaks were assigned based on the chemical structure of the analyte and literature reports. The letters (*s*, *b*, *w*, *sc*, *r*, *t*) after each chemical bond are used to indicate the vibrational mode, such as *s* = stretching, *b* = bending, *w* = wagging, *sc* = scissoring, *r* = rocking, and *t* = twisting.

Principal component analysis (PCA), a linear dimensionality reduction method, was employed to transform the original dataset into a smaller set of variables while preserving most of the information from the larger set. This technique was utilized in this study to differentiate the SERS signals of various analytes, including meropenem and its degradation products.

The limit of detection (LOD) was obtained by using measurements (n=15) at different concentrations, based on a linear regression trend between the signal and concentrations, within the employed concentration range. LOD is calculated as the concentration that corresponds to 3 times the standard deviation on the experimental calibration curve, relative to the slope of the linear regression.[6, 7]

Detecting carbapenemase activity

SERS detection. An experimental protocol was developed, as shown in Scheme 1, to detect the hydrolysis of meropenem in the presence of isolated carbapenemase or carbapenemase-producing bacteria. For the enzymatic reaction, the meropenem

solution (10 mg/L) was mixed with the selected purified carbapenemase (KPC-2 or OXA-48) at 5 μM and incubated for 45 min at room temperature. The mixture was then passed through a 10 kDa molecular weight cutoff filter (Sartorius Vivaspin Turbo15) by centrifugation at 4,000 rpm for 5 min, separating the hydrolysis products from the carbapenemases. The filtered solution was then applied to the SERS active substrate and measured with the IDRaman micro-Raman spectroscopy system. For assays employing carbapenemase-producing bacteria, plate cultures were prepared by streaking test strains on 2TY agar plates (supplemented with 25 μg/mL chloramphenicol when needed), followed by overnight incubation at 37 °C without shaking. The following day, a bacterial suspension was prepared in water to an OD_{600} of 0.1. Meropenem was added to this suspension to 10 mg/L, and following a 30-minute incubation, the mixture was passed through a 0.22 μm filter to separate bacterial cells from the carbapenems and carbapenem-derived products. Note that the meropenem concentration was chosen to ensure that measurable hydrolysis had occurred and was not related to the minimum inhibitory concentrations for meropenem against the CPO and non-CPO strains tested.[3]

UV-Vis spectrophotometric detection. Plate cultures of *E. coli* BW25113 (either untransformed or transformed with pACYC184-KPC-2) were prepared on 2TY agar (supplemented with 25 μg/mL chloramphenicol when needed) and grown overnight at 37 °C without shaking. The following day, bacterial suspensions were prepared in water to an OD_{600} of 0.1, and 100 μL of suspension was added to 100 μL of 20 μg/mL meropenem in a 96-well plate (Greiner Bio-One UV Star, flat bottom, clear). This resulted in a final bacterial OD_{600} of 0.05 and a meropenem concentration of 10 μg/mL. Absorbance readings at 297 nm were taken every 30 s for 30 min using a Synergy LX multimode plate reader.

Table S1. SERS peak analysis of meropenem and its hydrolyzed product.

Raman shift observed in meropenem (cm^{-1})	Raman shift observed in hydrolyzed meropenem (cm^{-1})	Assignment*	Reference
574	562	O–H *b* in carboxyl group	[8]
	780	C–N *s* in dimethylcarbamoyl group	[9]
880, 914		β-lactam breathing	[8, 9]
1000	1077	C–H *t/w* in trans-hydroxyethyl group C=O symmetric *s*	[8, 9]
1143		C–H *t* in dimethylcarbamoyl group C–N *s* in pyrrolidine	[8]
	1217	C–O–H *b* in carboxyl group	[9]
1250		C–N *s* in dimethylcarbamoyl group	[10]
	1356	C–H *w* in trans-hydroxyethyl group C–H *w* in pyrrolidine	[8]
1443		C–N *s* in pyrroline ring C–H *sc/w* in dimethylcarbamoyl group	[8, 10]
1500		C–H *s*	[9]
	1605	C=N *s* in pyrroline ring	[11]
	1668	C=O *s* in amide group or amide I vibration	[12]

Table S2. SERS peaks observed in Figures 2 and S4 which align with reported data for KPC-2 and OXA-48.

Raman shifts from KPC-2 (cm^{-1})	Raman shifts from OXA-48 (cm^{-1})	Reference
	714	[13]
938		[14]
	940	[13]
969		[14]
	1053	[13]
1109		[14]
1209		[14]
	1344	[13]
1378		[14]
	1558	[13]

* The letter after each chemical bond indicates the vibrational mode: *s* stretching, *b* bending, *w* wagging, *sc* scissoring, and *t* twisting.

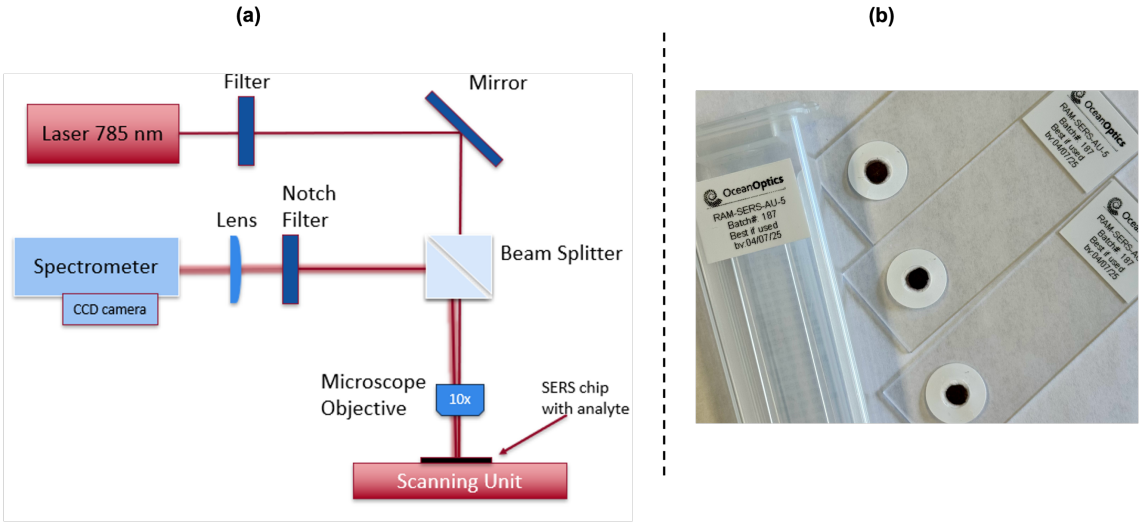

Figure S1. (a) Schematic of the optical setup, the IDRaman micro system, used for the acquisition of SERS spectra. (b) SERS substrate used in this study (Ocean Optics-RAM-SERS-AU-5).

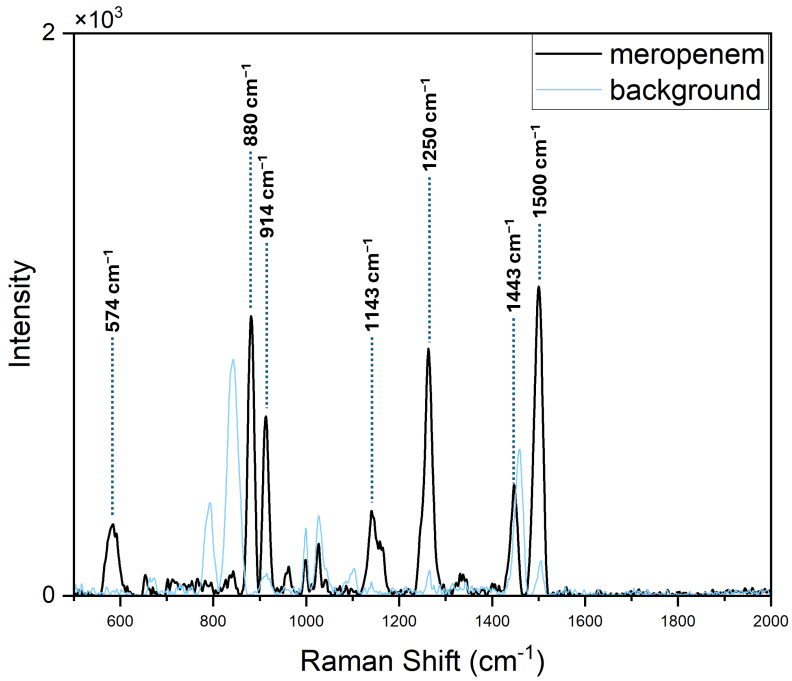

Figure S2. SERS spectrum of meropenem (10 mg/L aqueous solution) compared to a blank (Milli-Q® water).

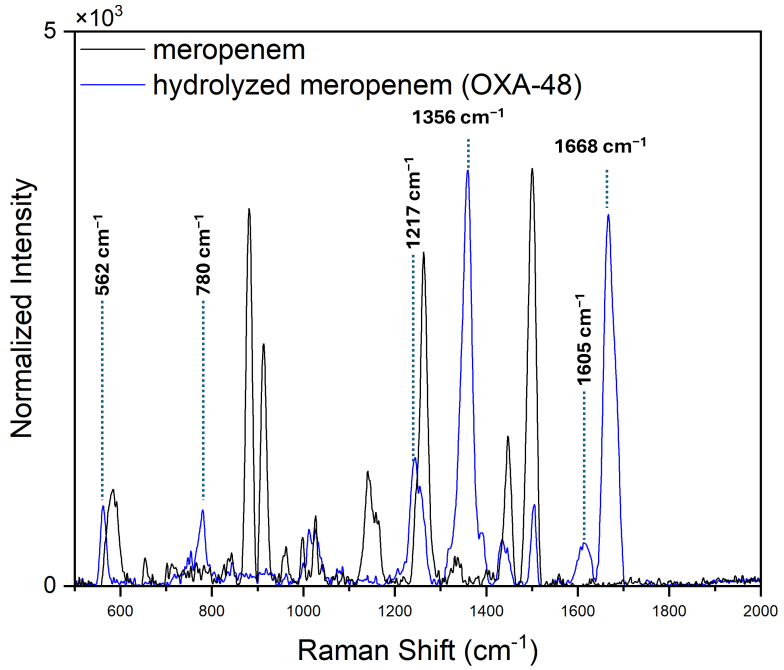

Figure S3. SERS spectra of meropenem and the meropenem-derived products formed by the carbapenemase OXA-48. The imine tautomer of the hydrolysis product is expected to be the major meropenem-derived species that is present.[15] Although OXA-48 has been reported to generate lactone products,[16] no distinct peaks corresponding to this product were observed in the SERS spectra.

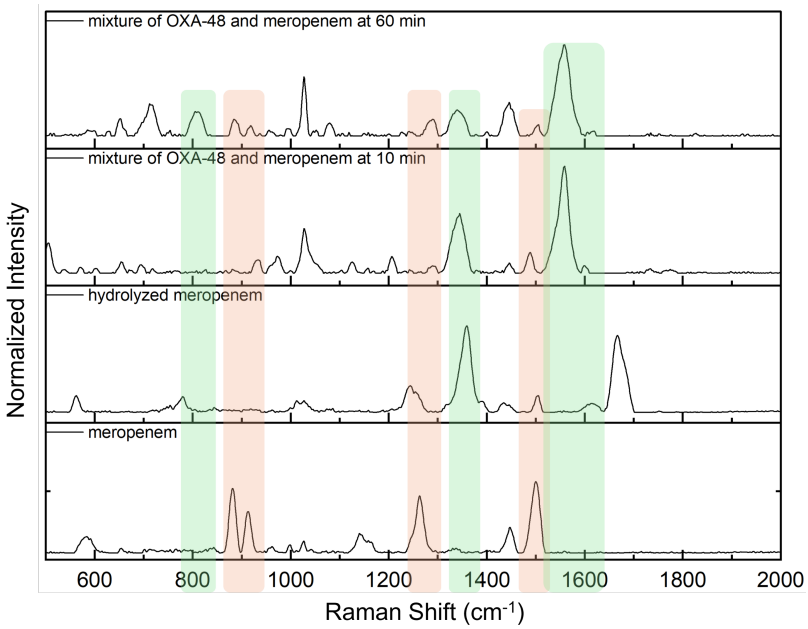

Figure S4. Monitoring a mixture of meropenem and OXA-48 at different time intervals using SERS. Red bands highlight disappearing peaks of meropenem, and green bands show new peaks corresponding to the hydrolysis

products. Note that longer incubation time points were tested for OXA-48 than for KPC-2, as OXA-48 degrades meropenem relatively slowly.[17, 18]

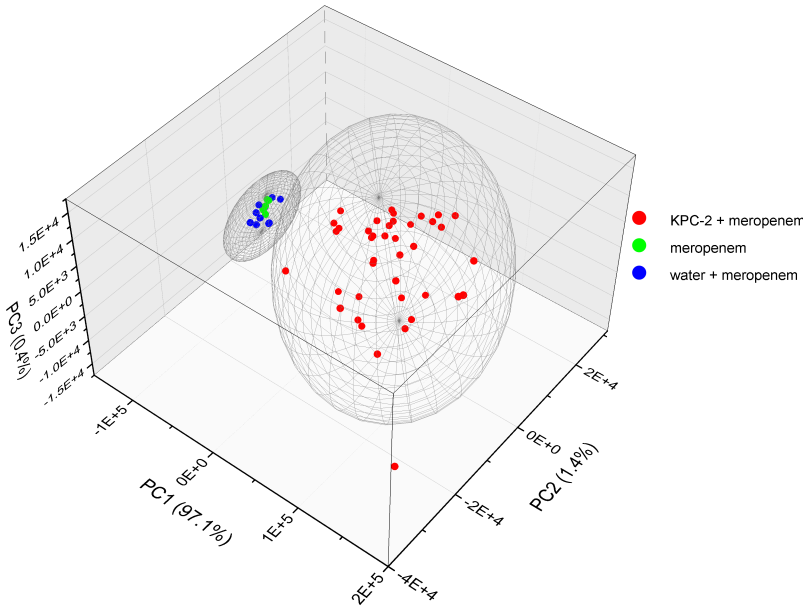

Figure S5. Score plot of principal component analysis (PCA) between meropenem, a mixture of meropenem with KPC-2, and meropenem stored as an aqueous solution at room temperature for 7 days. Spectral data sets for meropenem were collected from various spots on the substrate. Each dataset for the mixture of meropenem and KPC-2 was taken at different time intervals.

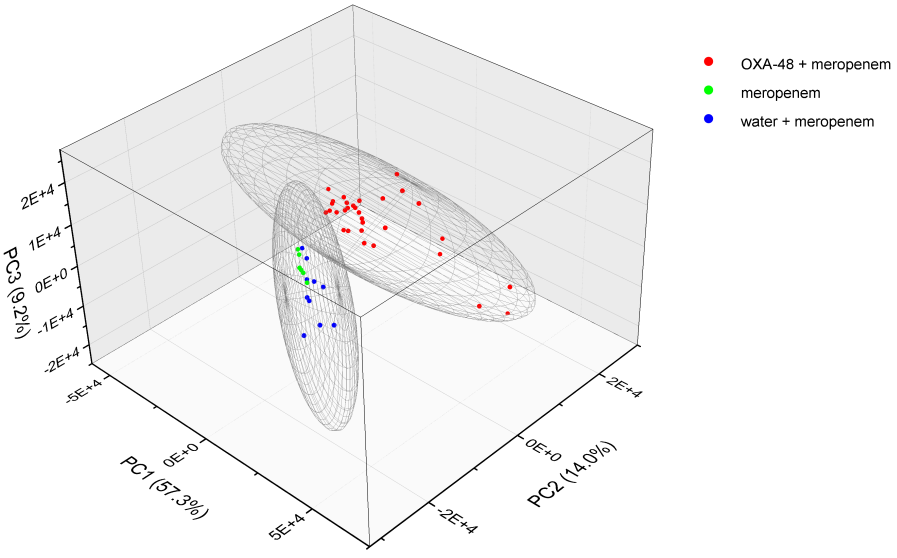

Figure S6. Score plot of principal component analysis (PCA) between meropenem, a mixture of meropenem with OXA-48, and meropenem stored as an aqueous solution at room temperature for 7 days. Spectral data sets for meropenem were collected from various spots on the substrate. Each dataset for the mixture of meropenem and OXA-48 was taken at different time intervals.

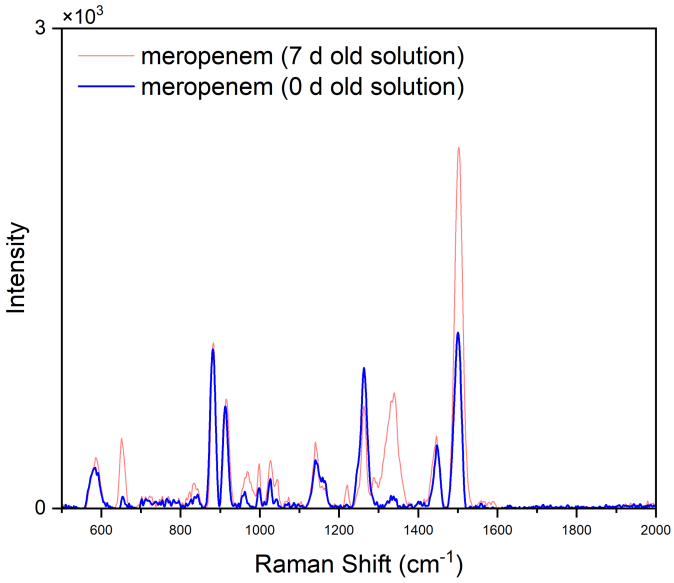

Figure S7. Stability of meropenem in water at room temperature. The major peaks are consistent between the two SERS spectra; the observed variations likely reflect that each spectrum is an average of multiple spectra acquired from different locations on the SERS substrate.

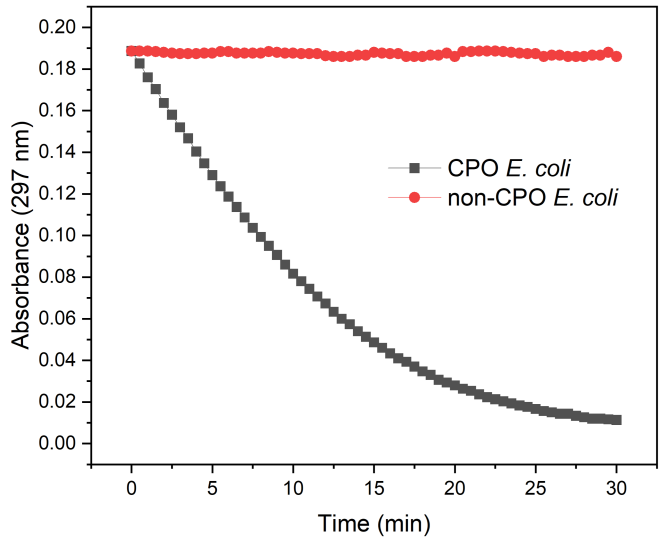

Figure S8. UV-Vis kinetic assay monitoring meropenem degradation (at λ = 297 nm) in the presence of CPO and non-CPO *E. coli* strains

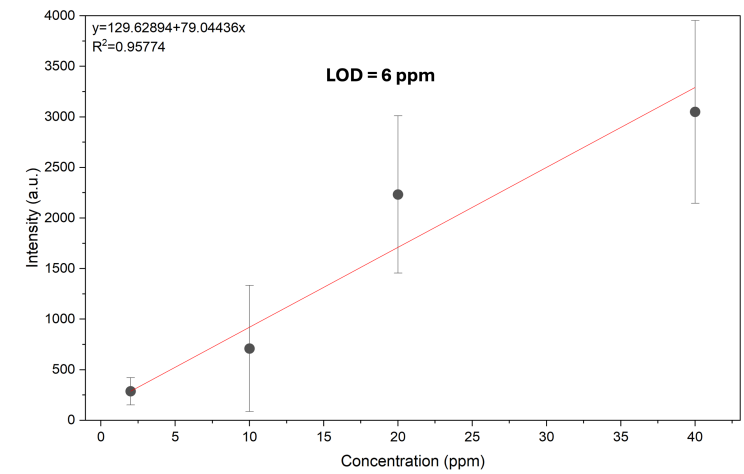

Figure S9. Calibration curve using linear fit across meropenem concentrations 2, 10, 20, and 40 ppm.

References:

1. S. T. Cahill, R. Cain, D. Y. Wang, C. T. Lohans, D. W. Wareham, H. P. Oswin, J. Mohammed, J. Spencer, C. W. Fishwick, M. A. McDonough, C. J. Schofield and J. Brem, *Antimicrob Agents Chemother*, 2017, **61**, 10.1128/aac.02260–02216.
2. C. L. Tooke, P. Hinchliffe, P. A. Lang, A. J. Mulholland, J. Brem, C. J. Schofield and J. Spencer, *Antimicrob Agents Chemother*, 2019, **63**, 10.1128/aac.00564–00519.
3. M. A. Jeffs, R. A. V. Gray, P. M. Sheth and C. T. Lohans, *Chem Commun (Camb)*, 2023, **59**, 12707–12710.
4. https://www.oceanoptics.com/accessories/sampling-accessories/
5. V. Snitka, D. Batiuskaite, I. Bruzaite, U. Lafont, Y. Butenko and C. Semprimoschnig, *CEAS Space J*, 2021, **13**, 509–520.
6. J. Vial and A. Jardy, *Analytical Chemistry*, 1999, **71**, 2672–2677.
7. H. Dies, J. Raveendran, C. Escobedo and A. Docoslis, *Sensors and Actuators B-Chemical*, 2018, **257**, 382–388.
8. S. Muneer, D. K. Sarfo, G. A. Ayoko, N. Islam and E. L. Izake, *Nanomaterials (Basel)*, 2020, **10**, 1756.
9. J. Cielecka-Piontek, M. Paczkowska, K. Lewandowska, B. Barszcz, P. Zalewski and P. Garbacki, *Chem Cent J*, 2013, **7**, 98.
10. V. P. Anjos, C. Marangoni, R. Nadas, T. N. Machado, D. Krul, L. S. Rodrigues, L. M. Dalla-Costa, W. H. Schreiner, D. M. Zezell, A. G. Bezerra, Jr. and R. E. de Goes, *Antibiotics (Basel, Switzerland)*, 2024, **13**, 1157.
11. C. Liu, C. Franceschini, S. Weber, T. Dib, P. Liu, L. Wu, E. Farnesi, W. S. Zhang, V. Sivakov, P. B. Luppa, J. Popp and D. Cialla-May, *Talanta*, 2024, **271**, 125697.
12. D. Kurouski, T. Postiglione, T. Deckert-Gaudig, V. Deckert and I. K. Lednev, *Analyst*, 2013, **138**, 1665–1673.
13. S. G. Sagdinc and A. Esme, *Spectrochim Acta A Mol Biomol Spectrosc*, 2010, **75**, 1370–1376.
14. G. Guo, C. Guo, X. Qie, D. He, S. Meng, L. Su, S. Liang, S. Yin, G. Yu, Z. Zhang, X. Hua and Y. Song, *Spectrochim Acta A Mol Biomol Spectrosc*, 2024, **308**, 123699.
15. C. T. Lohans, E. I. Freeman, E. V. Groesen, C. L. Tooke, P. Hinchliffe, J. Spencer, J. Brem and C. J. Schofield, *Sci Rep*, 2019, **9**, 13608.
16. C. T. Lohans, E. van Groesen, K. Kumar, C. L. Tooke, J. Spencer, R. S. Paton, J. Brem and C. J. Schofield, *Angew Chem Int Ed Engl*, 2018, **57**, 1282–1285.
17. S. C. Mehta, I. M. Furey, O. A. Pemberton, D. M. Boragine, Y. Chen and T. Palzkill, *J Biol Chem*, 2021, **296**, 100155.
18. V. Stojanoski, L. Hu, B. Sankaran, F. Wang, P. Tao, B. V. V. Prasad and T. Palzkill, *ACS Infect Dis*, 2021, **7**, 445–460.